AD/A-001 758

METALLURGICAL ASPECTS OF FRACTURE TOUGHNESS

A. J. McEvily

Connecticut University

Prepared for:

Air Force Office of Scientific Research

August 1974

UNCLASSIFIED

SECURITY CLASSIFICATION OF THIS PAGE *(When Data Entered)*

REPORT DOCUMENTATION PAGE		READ INSTRUCTIONS BEFORE COMPLETING FORM
1. REPORT NUMBER AFOSR - TR - 74 - 1698	2. GOVT ACCESSION NO.	3. RECIPIENT'S CATALOG NUMBER AD/A-001758
4. TITLE *(and Subtitle)* METALLURGICAL ASPECTS OF FRACTURE TOUGHNESS		5. TYPE OF REPORT & PERIOD COVERED INTERIM
		6. PERFORMING ORG. REPORT NUMBER UC-MET-3-1974
7. AUTHOR(s) A J MCEVILY		8. CONTRACT OR GRANT NUMBER(s) AFOSR-74-2703
9. PERFORMING ORGANIZATION NAME AND ADDRESS UNIVERSITY OF CONNECTICUT DEPARTMENT OF METALLURGY STORRS, CONNECTICUT 06268		10. PROGRAM ELEMENT, PROJECT, TASK AREA & WORK UNIT NUMBERS 681307 9782-05 6110F
11. CONTROLLING OFFICE NAME AND ADDRESS AIR FORCE OFFICE OF SCIENTIFIC RESEARCH/NA 1400 WILSON BLVD. ARLINGTON, VA. 22209		12. REPORT DATE AUGUST 1974 13. NUMBER OF PAGES 23
14. MONITORING AGENCY NAME & ADDRESS*(if different from Controlling Office)*		15. SECURITY CLASS. *(of this report)* UNCLASSIFIED 15a. DECLASSIFICATION/DOWNGRADING SCHEDULE

16. DISTRIBUTION STATEMENT *(of this Report)*

Approved for public release; distribution unlimited.

17. DISTRIBUTION STATEMENT *(of the abstract entered in Block 20, if different from Report)*

18. SUPPLEMENTARY NOTES

19. KEY WORDS *(Continue on reverse side if necessary and identify by block number)*

METALLURGICAL STRUCTURES
FRACTURE TOUGHNESS
DUCTILE FRACTURE
BRITTLE FRACTURE

20. ABSTRACT *(Continue on reverse side if necessary and identify by block number)*

In this paper a review of current topics of interest with respect to the interrelationship between microstructure and toughness is given. In the analytic treatments important parameters are particle size and spacing, the modulus, strength level and a measure of dutility. Metallurgical variables include mode of failure (cleavage, intergranular, transgranular), grain size, twins, temper embrittlement, slip mode, and sulfide morphology. Examples of the influence of these various factors on fracture toughness are given.

DD FORM 1 JAN 73 1473 EDITION OF 1 NOV 65 IS OBSOLETE

UNCLASSIFIED

SECURITY CLASSIFICATION OF THIS PAGE *(When Data Entered)*

Qualified requestors may obtain additional copies from the Defense Documentation Center, all others should apply to the National Technical Information Service.

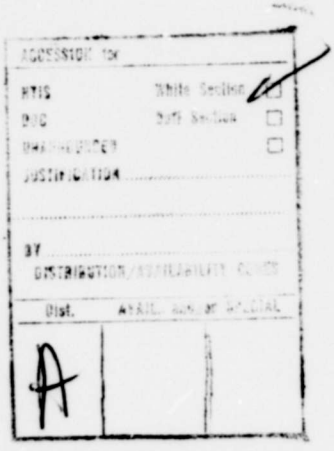

Conditions of Reproduction

Reproduction, translation, publication, use and disposal in whole or in part by or for the United States Government is permitted.

UC-Met-3-1974
August 1974
Interim Report
Contract AFOSR-74-2703

IMS

INSTITUTE OF MATERIALS SCIENCE

METALLURGICAL ASPECTS OF FRACTURE TOUGHNESS

A. J. McEvily

Approved for public release; distribution unlimited.

THE UNIVERSITY OF CONNECTICUT
Storrs · Connecticut

Metallurgical Aspects of Fracture Toughness

INTRODUCTION

The fracture toughness of an alloy is strongly dependent upon microstructure, but at present well established quantitative links between the two are lacking. As a result the field of fracture toughness remains semi-empirical in nature, with most of the quantitative aspects such as stress-intensity factors, plastic-zone sizes, and crack opening displacements being derived from continuum theory. However information of a qualitative nature is available on the role of microstructural features on fracture toughness, and it is a goal for the future to be able to establish improved quantitative interrelationships. In the present paper some of these known factors will be reviewed in order to bring out the current status of both the quantitative and the qualitative aspects of the interrelationship between fracture toughness and the microstructure.

Quantitative Approaches

The approach of Krafft[1] is of interest because it is an attempt to relate a microstructural feature to fracture toughness. He focuses attention on the ductile ligaments which form and bridge the crack tip region. These ligaments form about the largest non-continuous inclusions in the alloy. A correlation between the fracture toughness, K_{Ic}, and strain-hardening rate suggested that the tensile strain for ligament instability, ε_c, corresponded to the strain-hardening exponent, n. The initial ligament diameter, or process zone size, d_T, is estimated as the distance from the crack tip within which the tensile strain exceeded ε_c when K_I reached K_{Ic}. For small scale

yielding the tensile plastic strain at the crack tip up to the distance d_T is assumed to be uniform, and beyond d_T to fall off as in the elastic solution:

$$\varepsilon(\text{at and beyond } d_T) = \frac{K_I}{E\sqrt{2\pi d}} \qquad (1)$$

At the critical value of K_I, with ε equal to the strain hardening exponent, n, the value of K_{Ic} can be expressed as

$$K_{Ic} = En\sqrt{2\pi d_T} \qquad (2)$$

The average spacing of sulfide inclusions has correlated well with the process zone predicted by the Krafft equation. Fig. 1 is a plot of the influence of sulfur content on fracture toughness for a 4345 steel[2]. For similar steels, Birkle, Wei and Pellisier[3] found that the average size of inclusion-nucleated dimples were in close correspondence to d_T as calculated by the Krafft equation. Nevertheless in other cases it has been found that the dimple dimension bore no relationship to the measured particle spacing. This suggests that particles of various sizes may not be equally involved in the fracture process and the presence of a few large ones may override and suppress the contribution of smaller ones.[4] This matter of hole growth from inclusions is clearly not settled, but a recent critical assessment of plastic hole-growth mechanisms for ductile fracture has been given by Thomasson.[5] He concluded that transverse hole growth is a minor effect in comparison to extensional growth in bringing about the conditions for the onset of internal microscopic necking at the root of a sharp notch as well as in bulk plastic flow processes. In aluminum alloys large (1μ-10μ) particles fail at low strains (1-2%) with final separation occurring by the coalescence of small voids formed in bands of intense shear between the cracked

large particles.[6][7] Rosenfield and Hahn[8] also deal with the importance of ligaments in affecting fracture toughness. They find that the fracture toughness depends upon (a) the extent of the heavily strained region ahead of the crack tip, (b) the size of the ligaments as related to the volume fraction of cracked particles, and (c) the work of rupturing the ligaments. An approximate analysis predicts K_{Ie} varies as the 1/6 power of the volume fraction, f_c, of cracked particles. This result is obtained by relating the crack opening displacement, COD, given as

$$COD \approx \frac{0.5K^2}{E\sigma_y} \tag{3}$$

to the ligament width d_T, so that

$$K_{Ic} = \sqrt{2\sigma_y E d_T} \tag{4}$$

where σ_y is the yield strength. In terms of the volume fraction, f_c, and diameter of cracked particles, D,

$$K_{Ic} \approx \left[2\sigma_y E \left(\frac{\pi}{6}\right)^{1/3} D\right]^{1/2} f_c^{-1/6} \tag{5}$$

This relationship appears to be in good agreement with data on steels and high strength aluminum alloys, Fig. 2.

Peel and Forsyth[9] have developed a somewhat different expression for fracture toughness, in which the plastic work done in a small plastically deformed zone at the crack tip depends upon (1) the size of the zone, (2) the extent to which plastic deformation occurs before void formation causes fracture, and (3) the fracture stress. It is assumed that the distribution of plastic strain within the plastic zone is uniform although gradients in fact exist and also that the material obeys Ludwik's law ($\sigma = c\varepsilon^n$), so that the

plastic work in stretching a strip of height 2r to fracture is given as

$$G_{Ic} = \frac{2rC\ \varepsilon_f^{1+n}}{1+n} \tag{6}$$

where ε_f is the true strain at fracture. The expression for the fracture toughness becomes:

$$K_{Ic} = \sqrt{\frac{2ErC\ \varepsilon_f^{1+n}}{(1-\nu^2)(1+n)}} = \sqrt{\frac{2Er\ \sigma_f\ \varepsilon_f}{(1-\nu^2)(1+n)}} \tag{7}$$

A plot of experimental results in terms of the parameters of equation (6) is shown in Fig. 3. The slope of the lines should equal 2r, giving r values of 400, 90, and 40 μm to the three lines. The results suggest that intermetallic particles can control plastic zone size by the quantity present, but that orientation does not affect zone size but affects ε_f. It is surprising that the strip height in which plastic deformation is concentrated is apparently independent of the toughness level in a given alloy.

Another approach aimed at the identification of the relevant parameters involved in determining fracture toughness involves the use of the Neuber relationship[10]

$$K_T^2 = K_\sigma\ K_\varepsilon \tag{8}$$

where K_T is the theoretical stress concentration factor, K_σ is the stress concentration factor, and K_ε is the strain concentration factor. When localized plastic deformation occurs, K_σ decreases while K_ε increases, but the product remains constant, at least in approximation. Eq. (8) can be rewritten as

$$(K_T S)^2 = E\ \sigma_\ell\ \varepsilon_\ell \tag{9}$$

where S is the average applied stress, and σ and ε are interpreted to be the notch tip true stress and true strain respectively. Only small scale yielding is considered so that the bulk of the specimen is elastic. This equation can be related to the definition of the stress intensity factor

$$K = \lim_{\rho \to 0} \sigma_{max} \sqrt{\frac{\pi \rho}{4}} \tag{10}$$

but here we set $\rho \rightarrow \rho_e$, an effective radius for a fatigue crack, rather than to zero. The expression for fracture toughness becomes

$$K_{Ic} \approx \sqrt{\sigma_{\ell f} \, \varepsilon_{\ell f} \, E \rho_e} \tag{11}$$

This expression is similar to that of Forsyth and Peel, but with their plastic zone strip height replaced by an effective radius. It is noted that the lower values of the slopes of Fig. 3 corresponds to the order of the effective radii of fatigue cracks in aluminum alloys. In order to incorporate the effect of microstructure or toughness in this approach, the dependence of σ_ℓ, ε_ℓ, and ρ_e on microstructure needs to be established.

In comparing the four simplified approaches outlined above, it is seen that each shows a dependence of the fracture toughness on modulus. The Krafft model indicates that strain to necking is important, but does not include consideration of stress. The Hahn and Rosenfield model indicates that the toughness depends upon yield strength level but presents something of a problem since it is known that fracture toughness decreases with increase in yield strength. The Peel and Forsyth model as well as the fourth model both bring out the importance of both stress and strain on the toughness level, but obviously they are both over-simplified models. However the resultant expressions are intuitively of the proper form. It is also noted that if there is a critical value of COD for failure which can be expressed as the product of tip radius, ρ, and strain to failure, ε_f, then equation (3) results in the quantity $\sqrt{\sigma_y \, \varepsilon_f \, E\rho}$ being equal to K_{Ic}. These models could be indirectly related to the microstructure by expressing ε_f in terms of the volume fraction of second phase particles. As shown by Edelson and Baldwin[11] the tensile ductility varies inversely with the volume fraction of second phase

particles and voids. The influence of particles on ductility is also shown in Fig. 4 which is a plot of the stress-strain curves of air melted (ε_f = 0.9) and vacuum melted steel (ε_f = 1.2) of low carbon content.[12] These alloys differ only in elongation to failure; yield stress, strain hardening and necking strain being the same. Yet this is a most important difference, for Fig. 5 shows a much higher toughness level associated with the alloy of higher ε_f.[12] In this instance it has been possible to isolate a critical variable, and the result indicates that strain beyond necking can be important. However, elongation as determined in a simple tensile test may be misleading in certain cases, for Clausing[13] has pointed out that since in a given alloy system, fracture toughness decreases as the yield strength increases (for example, see Figs. 6, 14, and 7), that there should be a corresponding decrease in the tensile ductility. However as shown in Fig. 8[13], the round-bar tensile ductility was insensitive to yield strength for the steels he studied. However, when the tensile ductility was measured in a plane-strain tensile test, the expected decrease in elongation was observed, Fig. 8. It appears therefore that the plane strain ductility may be more meaningful with respect to fracture toughness as it more closely approximates the plastic flow pattern present at a crack tip. For any correspondence to exist between tensile ductility and fracture toughness it is also necessary that the fracture appearance be the same in both cases.[16]

Qualitative Aspects

The foregoing discussion has treated of macroscopic concepts and the role of particles in fracture. In this section some of the metallurgical factors will be discussed in more detail. The microstructure can have an

important influence in the degree of anisotropy and the mode of fracture, as indicated in Fig. 9.[9] In aluminum alloys fracture can be transgranular or intergranular, and in steels the additional fracture mode of cleavage can occur. Any low ductility mode, of course, results in a low value of toughness and is therefore to be avoided if possible. Intergranular modes are produced by the presence of grain boundary precipitates and by the segregation during heat treatment to grain boundaries of deleterious elements such as phosphorous in steels. In aluminum alloys the amount of grain boundary precipitates in underaged alloys results in a higher toughness than for overaged alloys at a given strength level, Fig. 10.[17]

At low temperatures, cleavage cracking in steels has been recognized to be a problem for some time. Fig. 11[18] indicates the trend of yield and fracture levels as a function of temperature. In the lowest temperature range shown the yield and fracture stress are nearly equal, an indication that plastic deformation is required to trigger this mode of failure. Fig. 12[19] confirms this fact and also shows the grain size dependence of the yield and fracture stress. Both of these stresses obey the Hall-Petch relation $\sigma_y = \sigma_i + k_y d^{-\frac{1}{2}}$ where σ_i is a friction stress, k_y is a material constant, and d is the grain size.

The temperature grain size dependency of low-carbon steels is shown schematically in a three dimensional plot, Fig. 13 . The important observation can be made from this figure that a decrease in grain size results in both increase in yield strength as well as a decrease in transition temperature (defined here as the temperature below which the yield and fracture stresses are the same). A reduction in grain size through controlled

rolling and cooling is an important industrial process to improve the properties of a steel without necessitating a change in composition. It is of interest that only a reduction in grain size can affect positively both the yield and the toughness levels.

Fig. 13 can also be used to visualize the influence of radiation embrittlement, strain rate, and notches on the transition temperature. Since embrittlement, an increase in strain rate, or the introduction of a notch will serve to increase the local yield stress, the intersection of the yield stress line, AC, with the fracture line, CE, will occur at a higher temperature, with the result that the transition temperature is increased. An increase in inclusion content will lower the fracture stress line CE, and also cause an increase in transition temperature. With respect to grain size, a change from wavy to planar slip will increase the Hall-Petch slope and reduce the transition grain size below which the yield stress is less than the fracture stress. Such a change will also result in an increase in transition temperature. The process of twinning or the pre-existence of twins in steels can have an adverse effect on fracture toughness, as indicated in Figs. 14[20] and 15[21]. In the latter case the carbides were not uniformly distributed in the twinned martensite, and the twin provided an easy path for fracture. The bainite was a more homogeneous structure with resultant increase in toughness at a given strength level. Thermal mechanical processing can also be used to improve the homogeneity of an alloy. Fig. 16[22] shows the range of improvement found by one combination of deformation and heat treatment.

Anisotropy can have an important effect in fracture toughness as in

Fig. 9. A recent development of interest involves the addition of rare earth metals to steel to influence the morphology of sulfide inclusions. These inclusions are responsible for much of the anisotropy in fracture toughness typical of plate products. As shown in Fig. 17[23] the shape is much more spherical and the particles less deformable than the sulfide stringers usually present. Fig. 18[24] shows how the rare earth additions can serve to minimize anistropy associated with these stringers.

In this paper on plots of fracture toughness as a function of strength level, a line along which $\left(\frac{K_{Ic}}{\sigma_y}\right)^2 = 2.5\text{mm}$ is shown which stems from the ratio analysis diagram (RAD) concept of Pellini. The use of this criterion arises from a combination of fracture mechanics and non-destructive inspection.[22] Consider a structure containing a crack of length 2a. The structure will fail when $K = \sigma\phi\sqrt{\pi a} = K_{Ic}$, where σ is the applied stress and ϕ is a function of geometry. Let the safely factor be α, i.e., $\sigma = \alpha\sigma_y$, thus

$$\left(\frac{K_{Ic}}{\sigma_y}\right)^2 = \phi^2\alpha^2\pi a. \qquad (12)$$

Eq. (12) defines the largest crack that the plate can safely contain, which should equal the largest crack that the inspection method will <u>not</u> detect. A typical value of α is 0.8, so that $\left(\frac{K_{Ic}}{\sigma_y}\right)^2 \approx 2a\phi^2$. For a through crack in a tensile loaded panel, $\phi = 1$ and $\left(\frac{K_{Ic}}{\sigma_y}\right)^2$ is just equal to the critical crack length which must be inspected out.[22]

To illustrate the interplay between toughness and safety, a schematic toughness/strength diagram is shown in Fig. 19. If the criterion of inspectability is that any crack longer than 2.5 mm wil be detected, alloys below the line will be unsafe and alloys above safe. Consider two alloys

which lie at points A and B. Note first that alloy B is tougher than alloy A. However, alloy B is not as safe, because critical cracks will escape detection. The obvious goal for this alloy is to increase the toughness to some level such as B', without sacrificing strength. For alloy A, the temptation might be to increase strength at no sacrifice in toughness. The result could be as represented by point A' in Fig. 19. In this case the 2.5 mm line is crossed and the safety of the structure is reduced below the established level. If alloy A is to operate safely at $\sigma = 0.8\sigma_y$ the inspection capability must be improved from 2.5 mm to 2.0 mm. If this is not possible, the allowable stress must be reduced to $\sigma = 0.72\ \sigma_y$ according to Eq. (12), cancelling out the benefits of increased strength. The lines of constant safety in Fig. 19 are the straight lines through the origin representing critical crack lengths. To improve alloy A and maintain its level of safety, strength and toughness must move along line A-A". These points must be kept in mind to insure that any apparent improvement is not at the expense of safety.

CONCLUDING REMARKS

From the metallurgical point of view the following microstructural characteristics are seen to enhance fracture toughness: homogeneity of structure, the absence of easily fractured particles and easy fracture paths, strong interfaces, wavy glide, and an abundance of mobile dislocations. In addition, when the microstructure leads to high strength, high levels of toughness are obtained as in the case of the maraging steels. In so far as they can be followed, these guidelines should serve to improve the toughness in other alloy systems as well.

References

1. Krafft, J. M., Appl. Mats. Res., 3, 1964, 88.

2. Wei, R. P., ASTM STP 381, 1965, 279.

3 Birkle, A. J., Wei, R. P. and Pellissier, G. E., ASM TRANS QUARTERLY, 59, 1966, 981.

4. Forsyth, P. J. E., AGARD Report R-610, 1973, 1.

5. Thomassen, P. F., in "Prospects of Advanced Fracture Mechanics", Delft, 1974, to be published.

6. Broek, D., ibid.

7. Low, J. F., ibid.

8. Rosenfield, A. R. and Hahn, G. T., Met. Trans., to be published.

9. Peel, C. J. and Forsyth, P. J. E., Met. Sci. J., 7, 1973, 121.

10. Neuber, H., J. Appl. Mech., ASME, 28, 1961, 544.

11. Edelson, B. and Baldwin, W., Trans. ASM, 55, 1962, 230.

12. McEvily, A. J., et. al., in "Transformation and Hardenability in Steels, Climax Molybdenum Co., 1967, 179.

13. Clausing, D. P., Technical Paper W9-15.3, ASM, 1969.

14. Burns, K. and Pickering, F., J. Iron and Steel Inst., 202, 1964, 899.

15. Zackay, V. F. et. al., Paper C2-35, Third Int. Conf. on Strength of Metals and Alloys, Cambridge, 1973.

16. Low, J. R., Private communication.

17. Develay, R., Metals and Materials, 6, 1972, 404.

18. Hahn, G. T. et. al., in "Fracture", John Wiley, New York, 1959, 91.

19. Low, J. R., in "Relation of Properties to Microstructure", ASM, Cleveland, Ohio, 1953, 163.

20. McMahon, J. A. and Thomas, G., Paper C2-36, Third Int. Conf. on The Strength of Metals and Alloys, Cambridge, 1973.

21. Liu, Y. H., ASM TRANS. QUARTERLY, 62, 1969, 55.

22. Rosenfield, A. R. and McEvily, A. J., AGARD Report-R-610, 1973, 23.

23. Bennett, H. W. and Sandell, L. P., J. Metals, 26, 1974, 21.

24. Luyckx et. al., Met trans., 1, 1970, 3341.

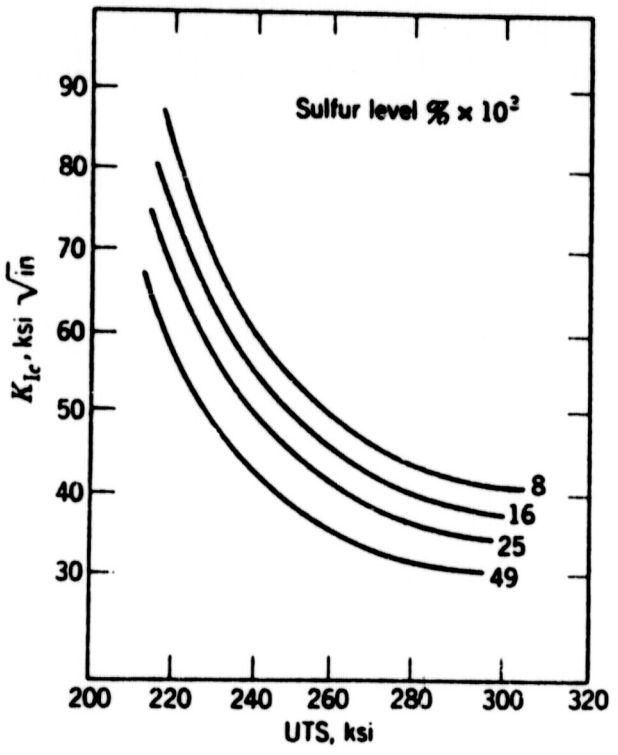

Fig. 1. Effect of tensile strength level and sulfur content on K_{Ic} for quenched and tempered 4345 steel. After Wei[2].

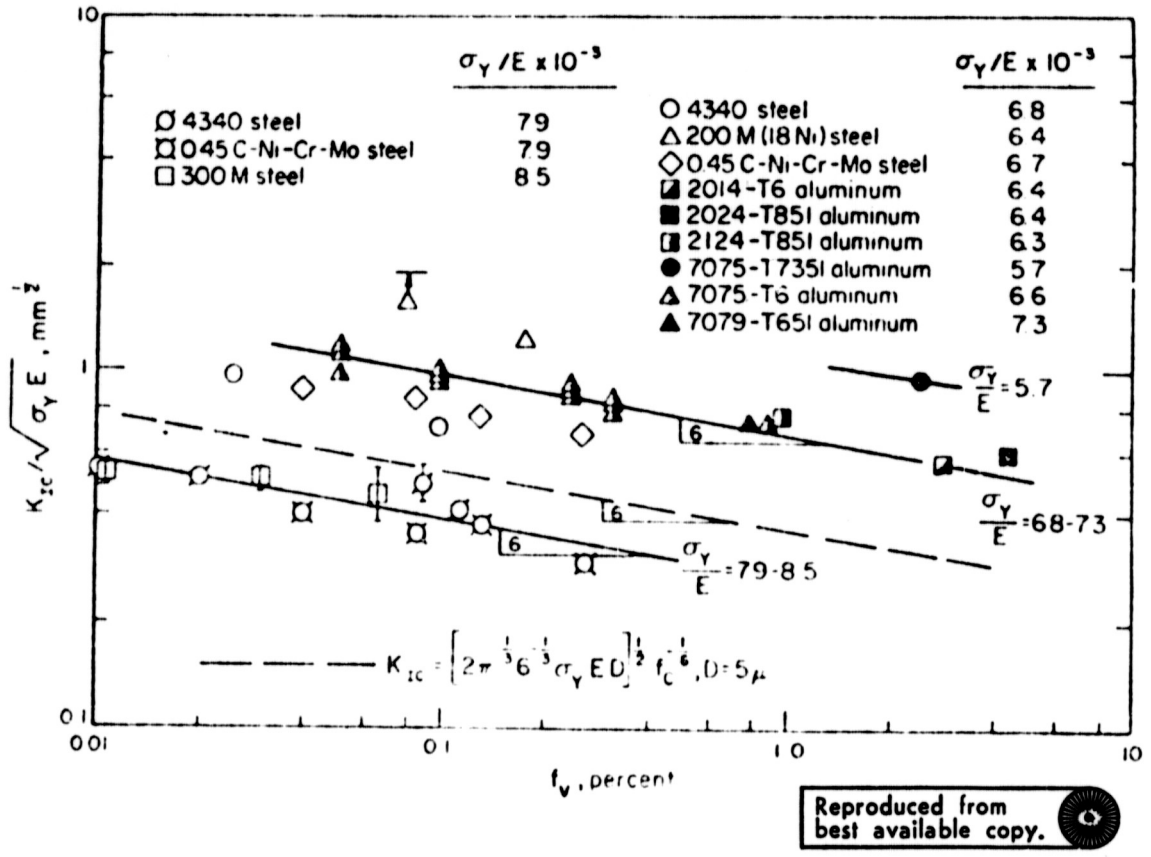

Fig. 2. Influence of volume fraction of large (>1μ size) second phase particles on the plane strain fracture toughness of commercial alloys. After Rosenfield and Hahn.[8]

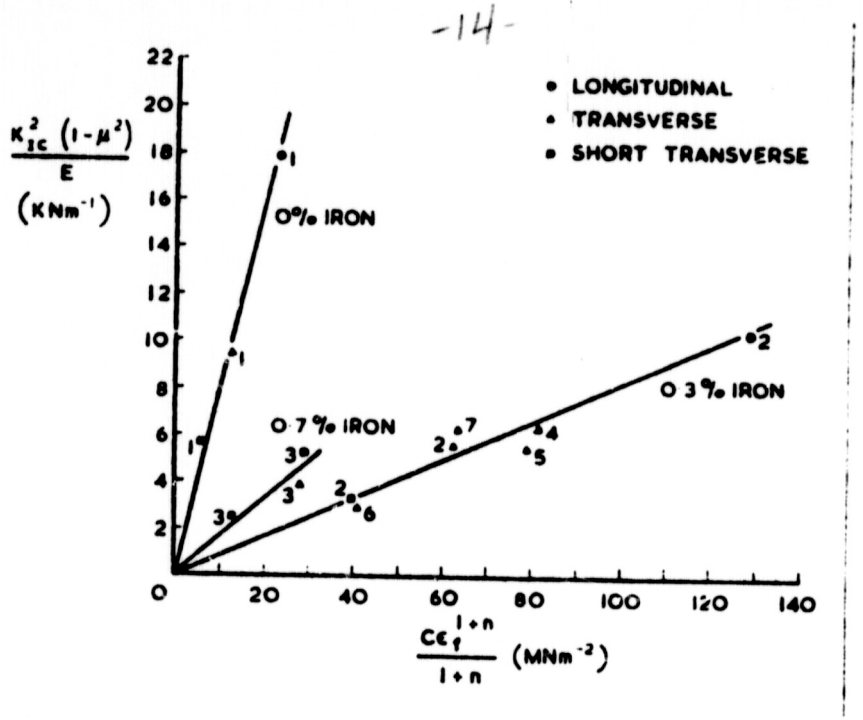

Fig. 3. A plot of energy-release rate vs. plastic work to fracture for seven Al-Zn-Mg-Cu-Mn forging alloys showing the effect of iron content and stress direction. After Peel and Forsyth[9].

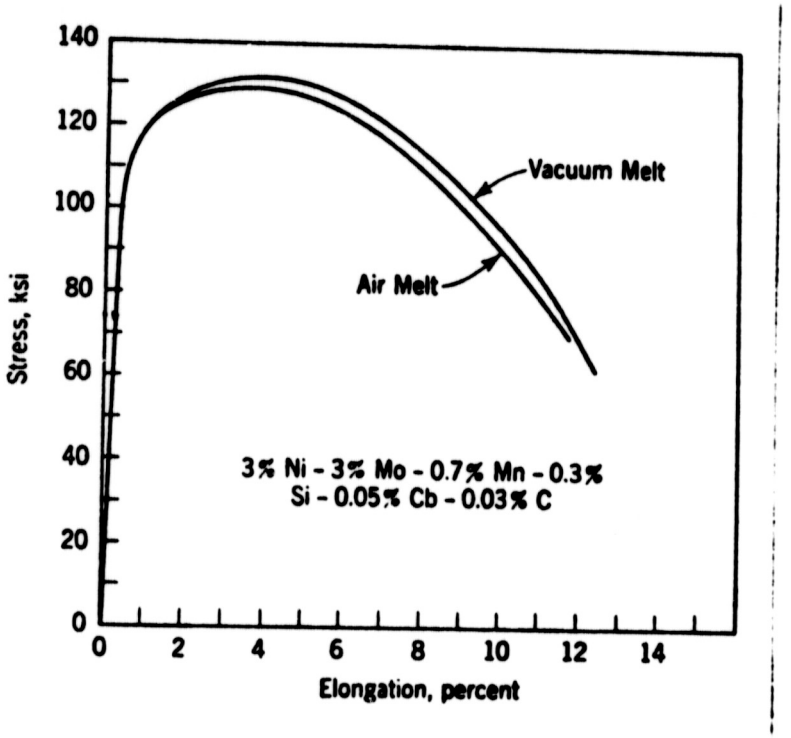

Fig. 4. Stress-strain curves for vacuum and air melted alloys of nominal composition 3Ni-3Mo-0.7Mn-0.3Si-0.03Nb. After McEvily et. al.[12]

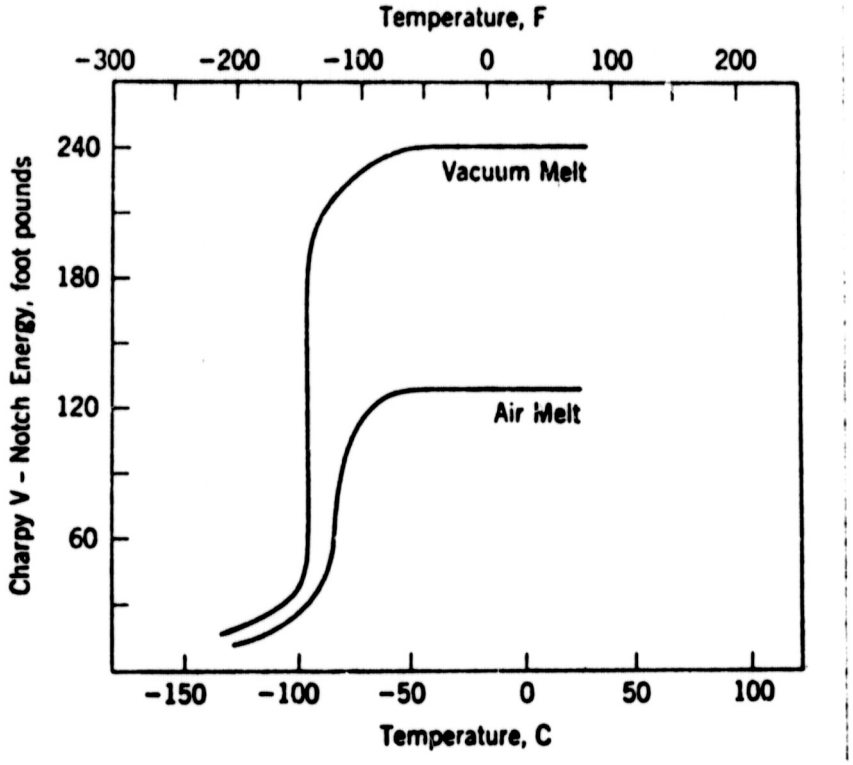

Fig. 5. Impact properties of vacuum and air melted 3Ni-3Mo steels.[12]

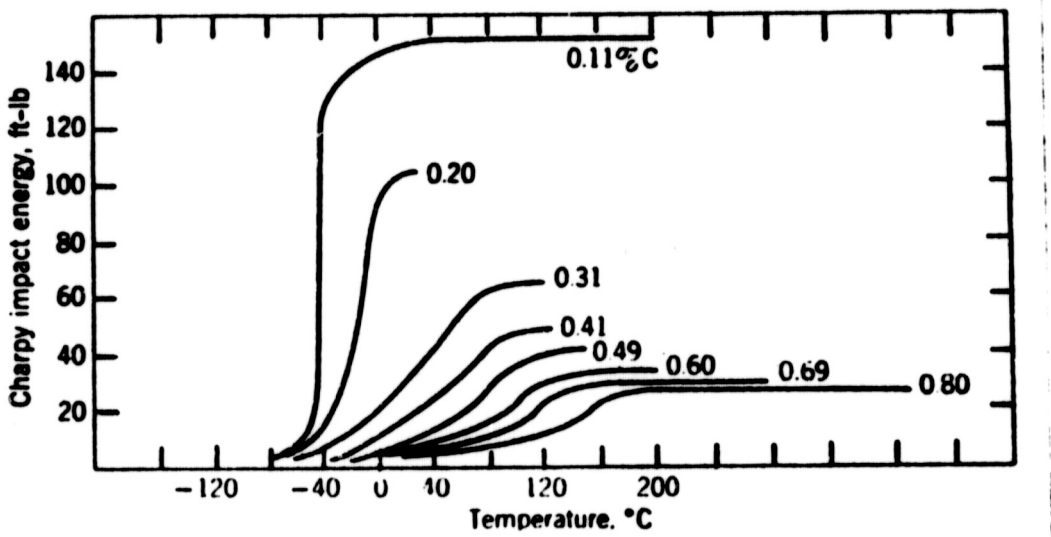

Fig. 6. Effect of Carbon content on the Charpy impact energy curves for normalized iron carbon alloys. After Burns and Pickering.[14]

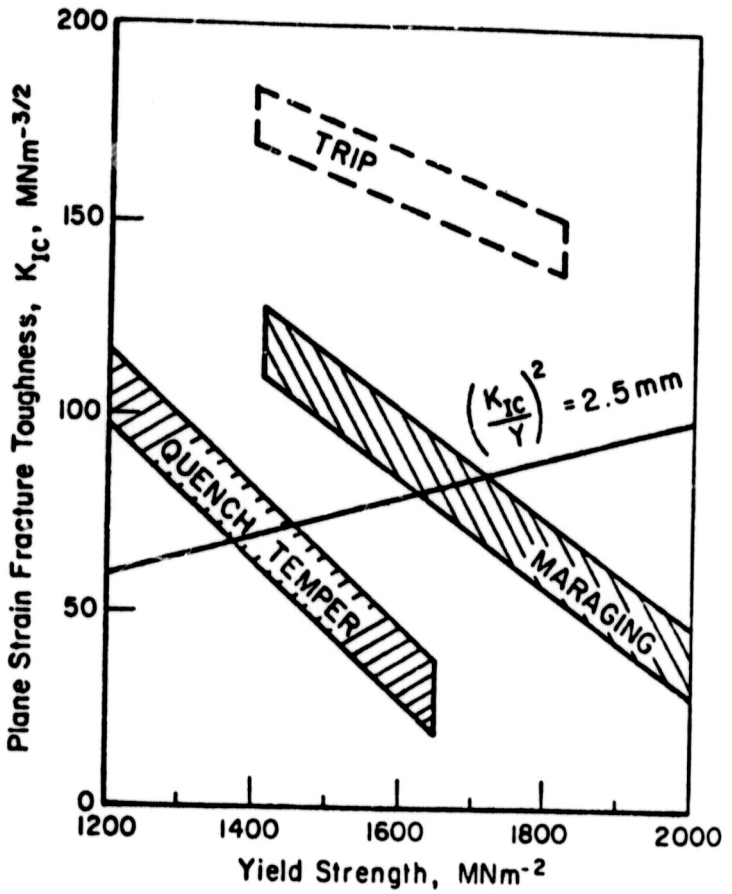

Fig. 7. Toughness-strength relations for steels. After Zackay et. al.[15]

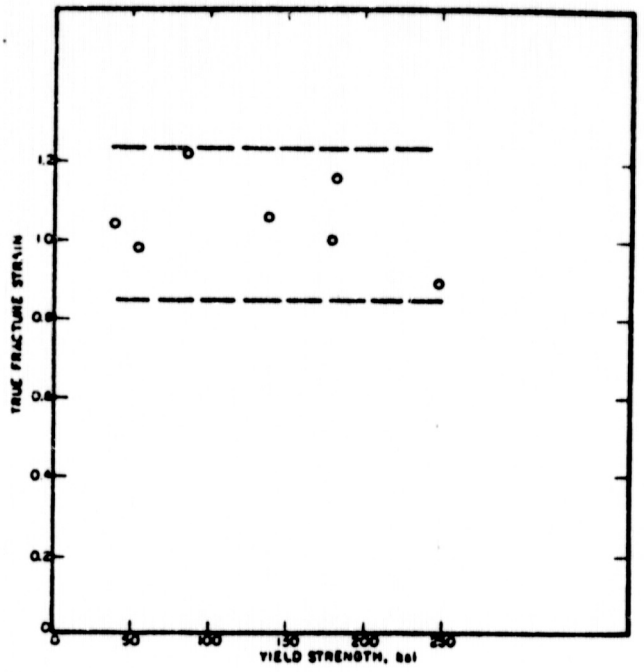

a

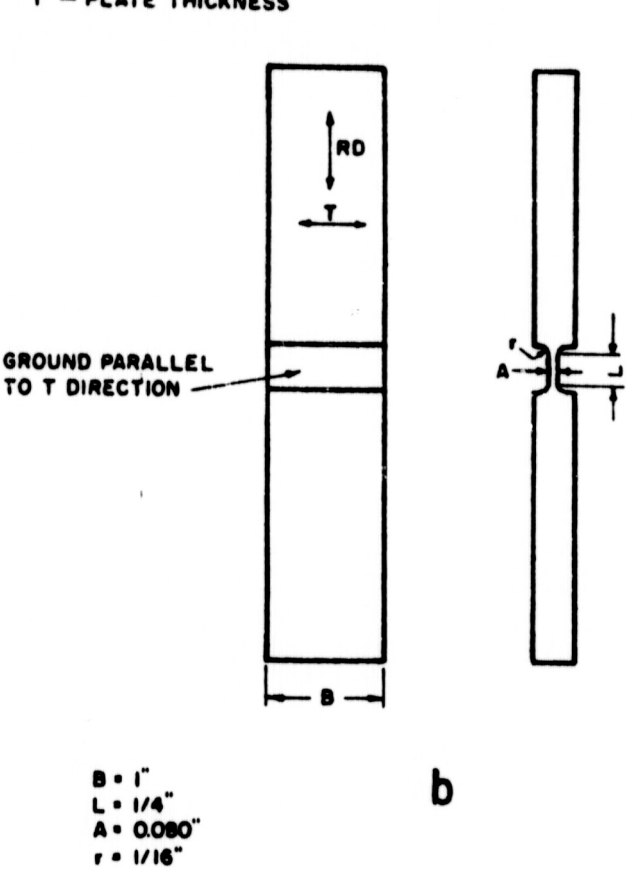

B = 1"
L = 1/4"
A = 0.080"
r = 1/16"

b

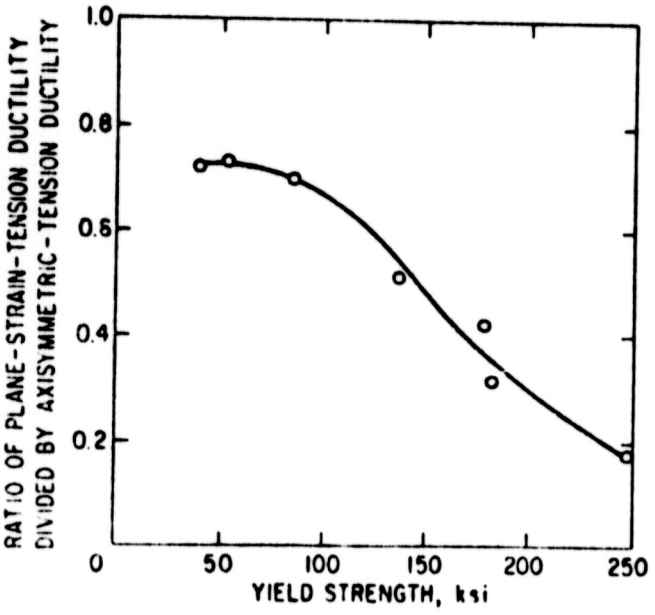

c

Fig. 8. Effect of tensile specimen shape on fracture strain. (a) Round tension bar results. (b) Plane-strain tension specimen. (c) Plain-strain tensile bar results. After Clausing.[13]

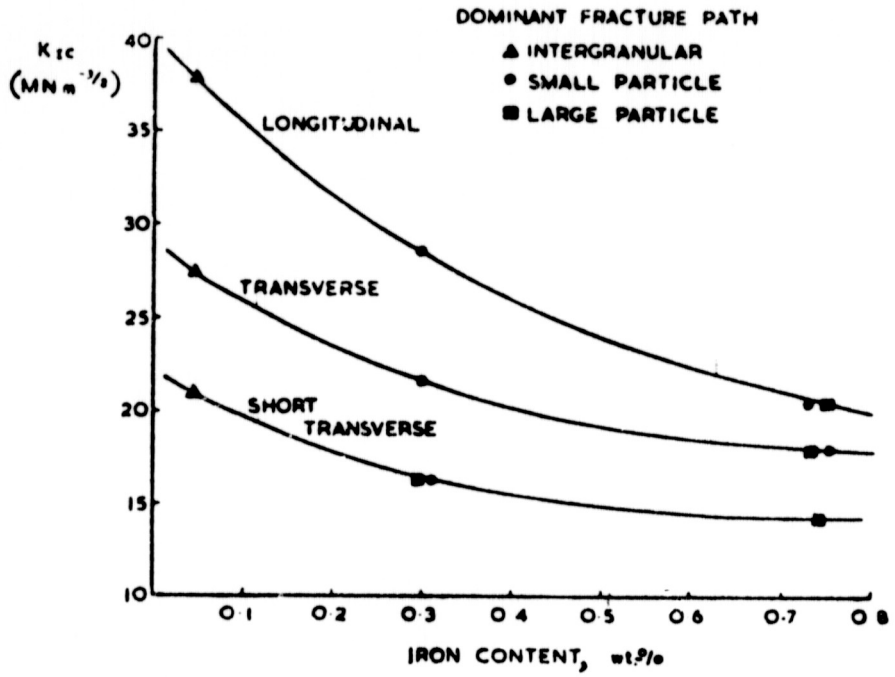

Fig. 9. Fracture toughness and fracture mode as a function of iron content in Al-Zn-Mg-Cu-Mn forging alloys. After Peel and Forsyth.[9]

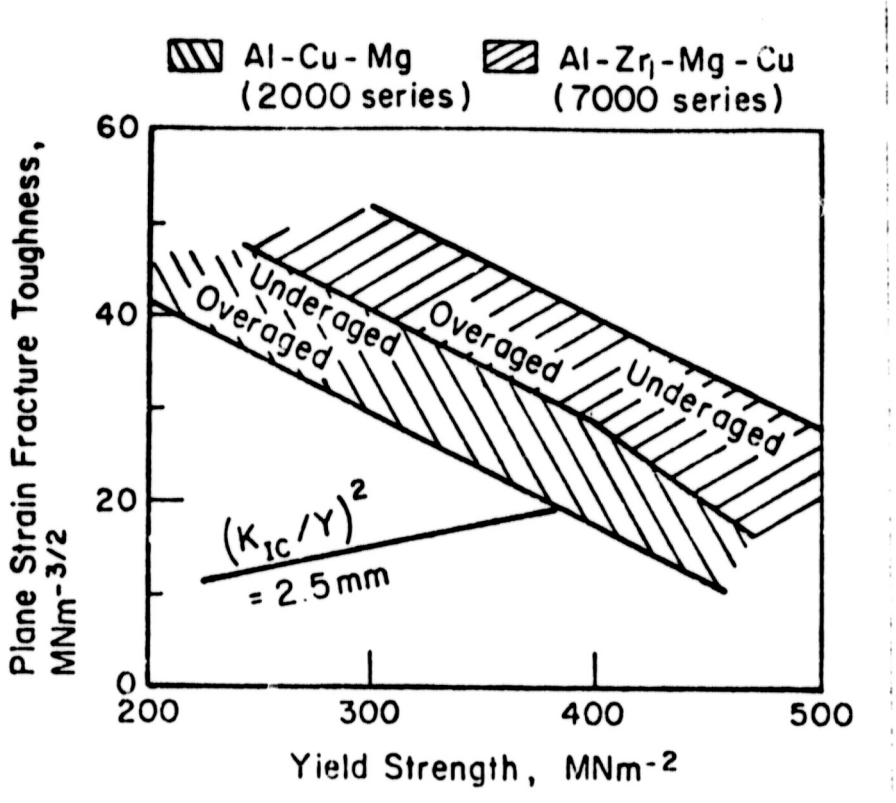

Fig. 10. Schematic diagram of strength-toughness relation for aluminum alloys. After Develay.[17]

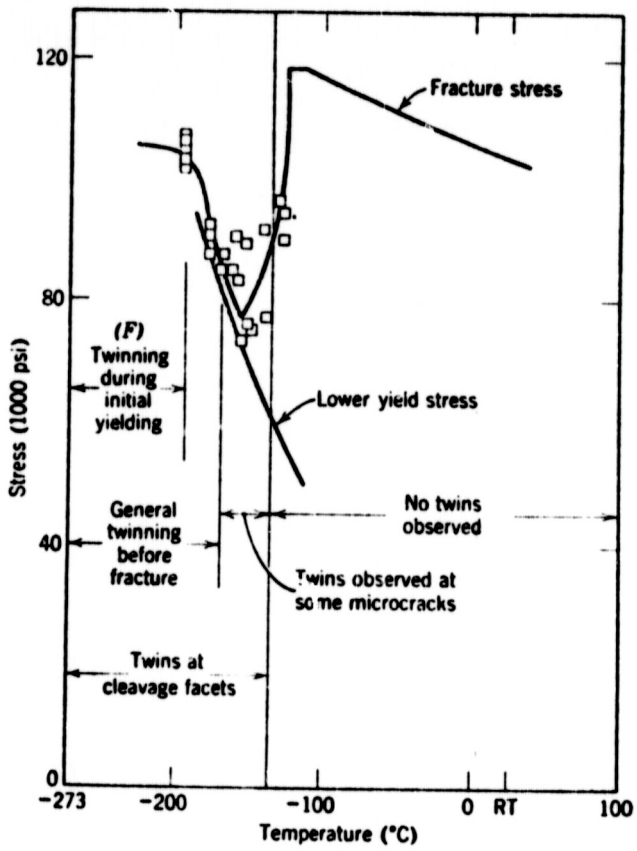

Fig. 11. Tensile properties as a function of temperature for coase-grained 0.22 Carbon Steel. After Hahn et. al.[18]

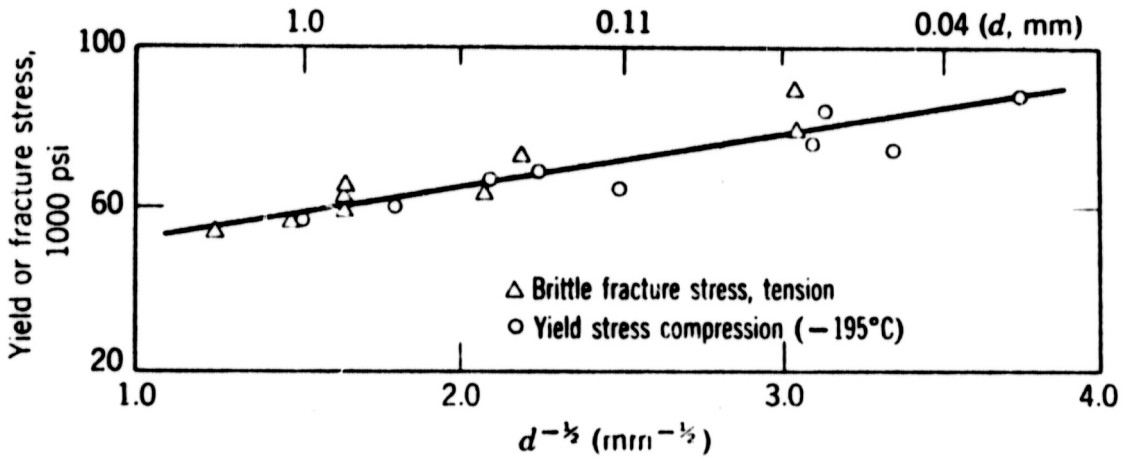

Fig. 12. Effect of grain size on yield stress and the fracture stress of polycrystalline iron at -195°C. After Low.[19]

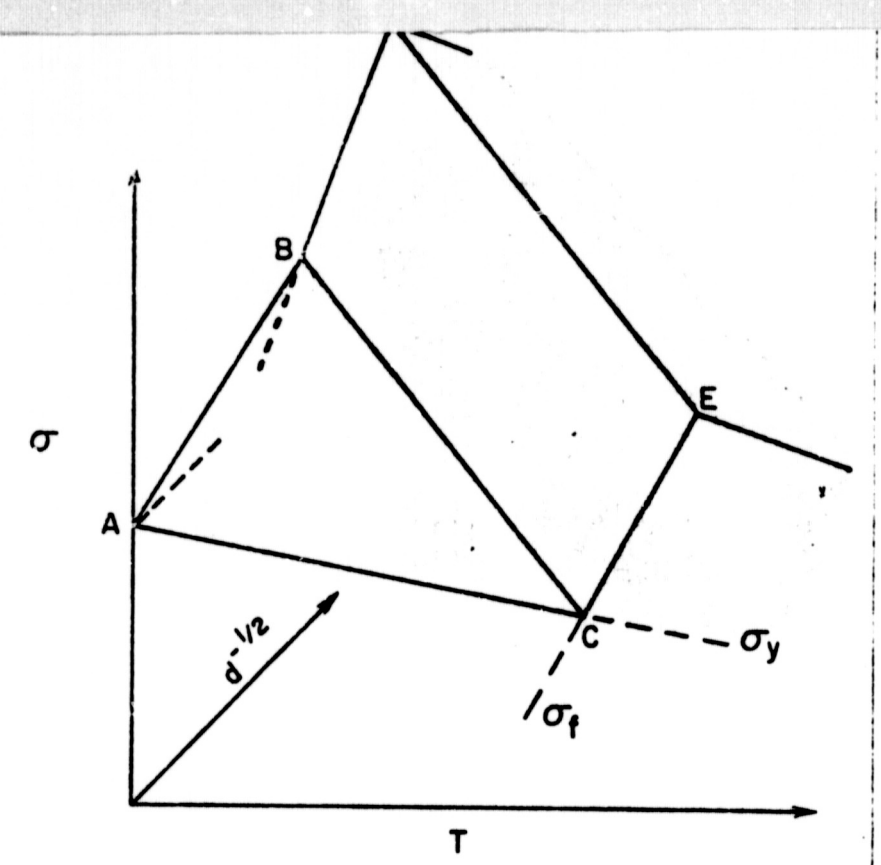

Fig. 13. Three dimensional stress-temperature - $d^{-\frac{1}{2}}$ plot. Cleavage initiated fractures to left of DE. ABC is a locus at which brittle fracture occurs when the applied stress reaches the yield stress.

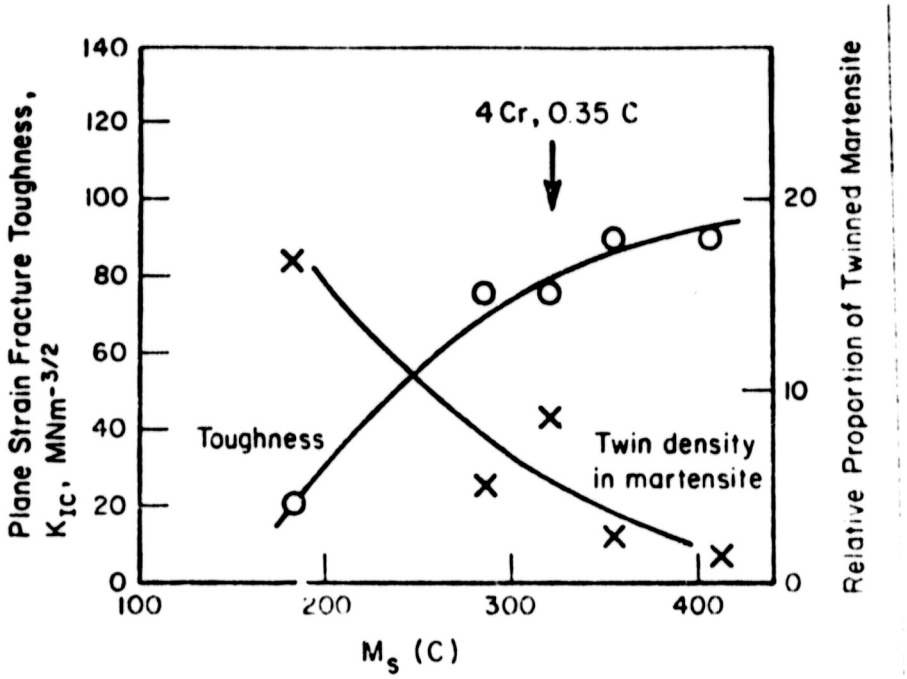

Fig. 14. Toughness and microtwin frequency as a function of martensite start temperature for a series of Fe-Cr-C alloys. After McMahon and Thomas.[20]

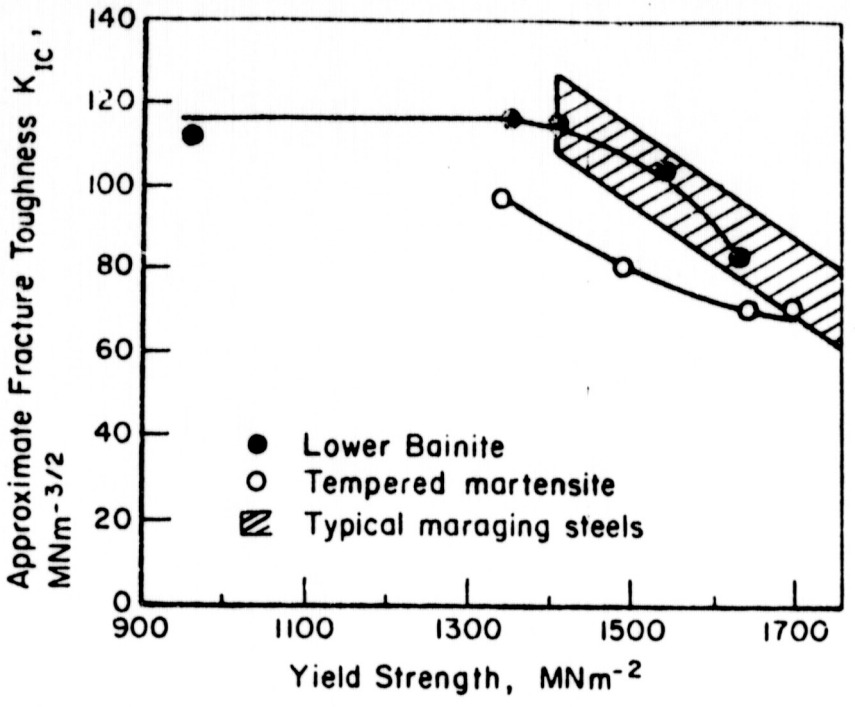

Fig. 15. Fracture toughness as a function of yield stress and microstructure for steel HP9-4-45 (8Ni-3.8Co-.43C). After Liu.[21]

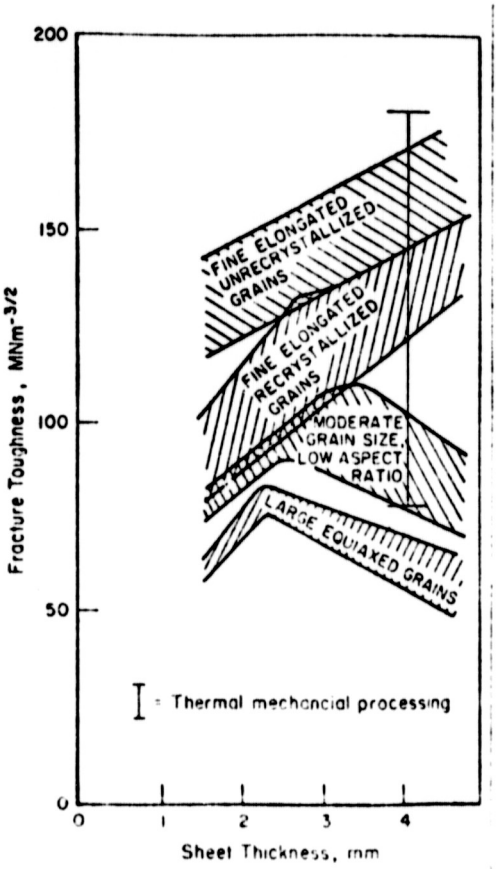

Fig. 16. Effect of sheet thickness and microstructure on the fracture toughness of overaged 7000 series aluminum sheet. The effect of thermal mechanical processing is also indicated. After Rosenfield and McEvily.[22]

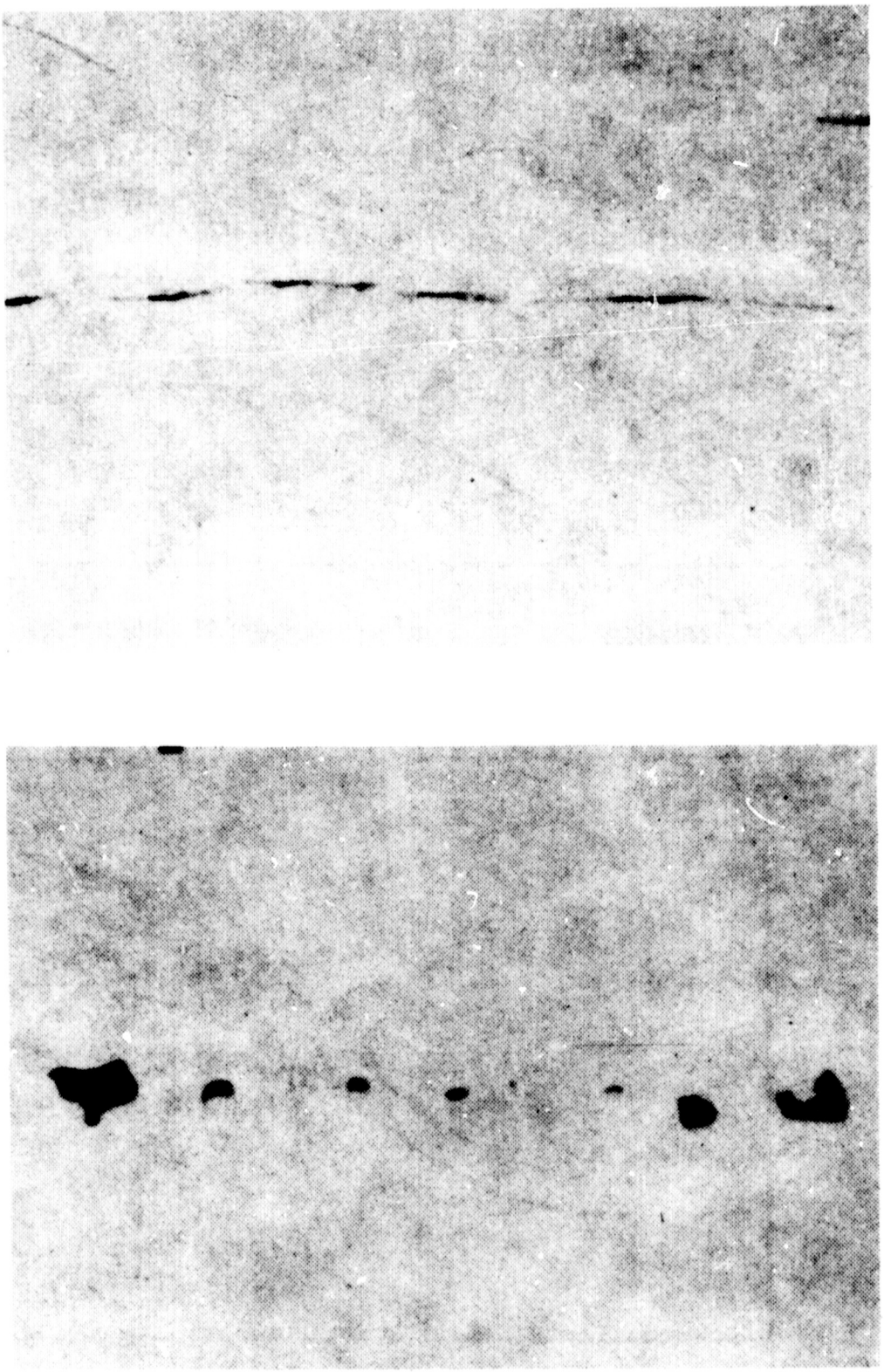

Fig. 17. Comparison of sulfide shape control. a) nontreated x1000, b) rare earth treated x1000. After Bennett and Sandell.[23]

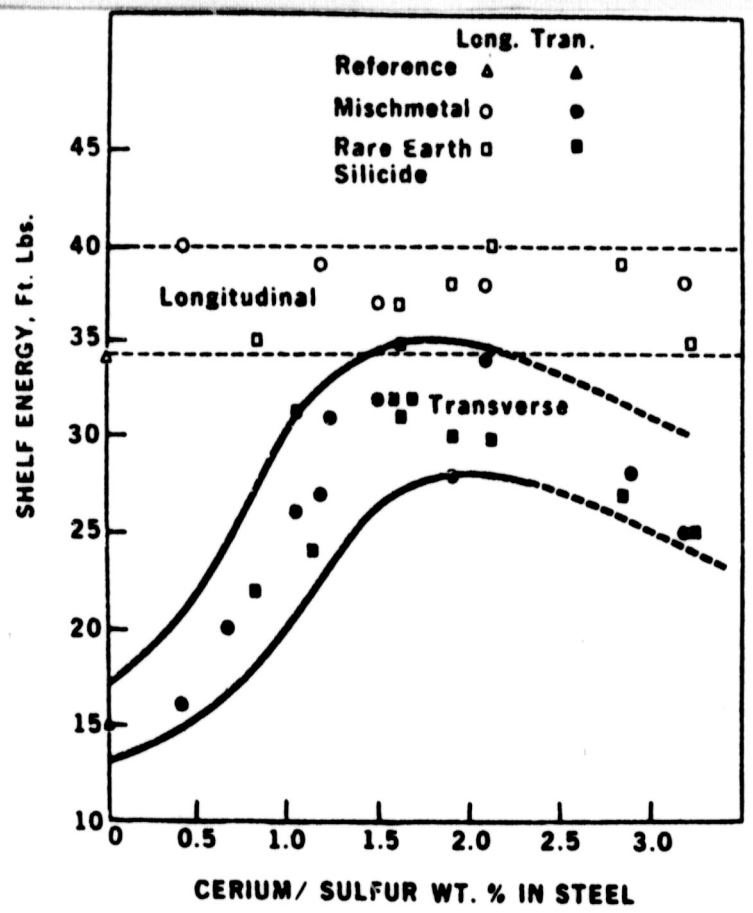

Fig. 18. Relationship between shelf energy determined on longitudinal and transverse Charpy ½ size V-notch specimens and cerium to sulfur ratio. Each data point is the average of two tests. After Luyckx et. al.[24]

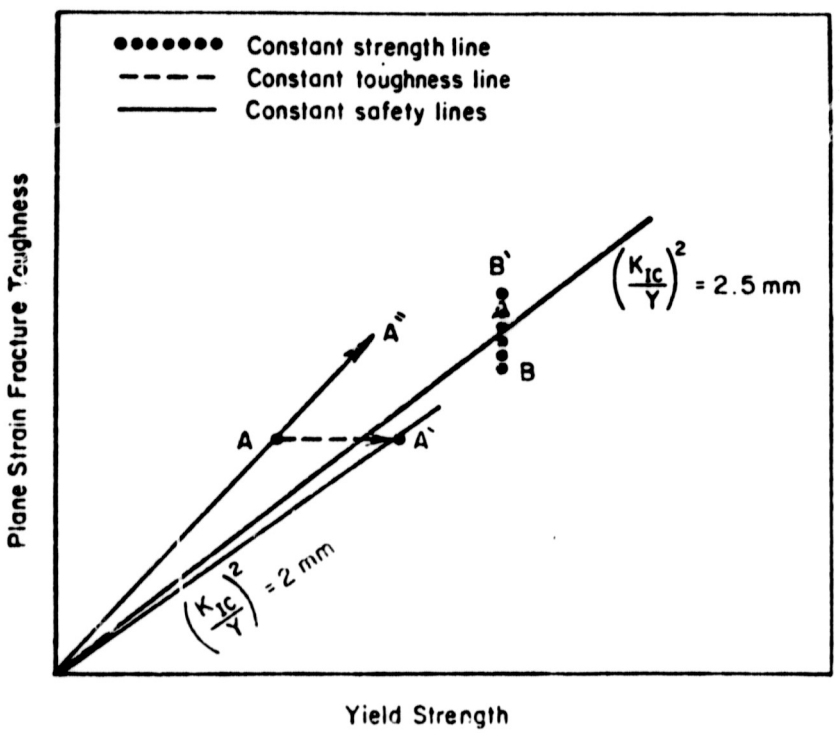

Fig. 19. Schematic toughness/strength diagram illustrating the concept of safety. After Rosenfield and McEvily[22]

INSTITUTE OF MATERIALS SCIENCE

The Institute of Materials Science was established at The University of Connecticut in 1966 in order to promote the various fields of materials science. To this end, the State of Connecticut appropriated $5,000,000 to set up new laboratory facilities, including approximately $2,150,000 for scientific equipment. In addition, an annual budget of several hundred thousand dollars is provided by the State Legislature to support faculty and graduate student salaries, supplies and commodities, and supporting facilities such as various shops, technicians, secretaries, etc.

IMS fosters interdisciplinary graduate programs on the Storrs campus and at present is supporting five such programs in Alloy Physics, Biomaterials, Crystal Science, Metallurgy, and Polymer Science. These programs are directed toward training graduate students while advancing the frontiers of our knowledge in technically important areas.